Dynamic Singularities in Cooperative Exclusion

Alan Gabel[1] and S. Redner[1]
[1] *Center for Polymer Studies and Department of Physics, Boston University, Boston, Massachusetts 02215, USA*

We investigate *cooperative exclusion*, in which the particle velocity can be an increasing function of the density. Within a hydrodynamics theory, an initial density upsteps and downsteps can evolve into: (a) shock waves, (b) continuous compression or rarefaction waves, or (c) a mixtures of shocks and continuous waves. These unusual phenomena arise because of an inflection point in the current versus density relation. This anomaly leads to a group velocity that can either be an increasing or a decreasing function of the density on either side of these wave singularities.

PACS numbers: 02.50.-r, 05.40.-a

The asymmetric exclusion process (ASEP) [1–6] paradigmatically describes transport in one-dimensional crowded systems, including traffic [7–10], ionic conductors [11], and RNA transcription [12, 13]. In the ASEP, each site of a one-dimensional lattice is either vacant or occupied by a single particle that can hop at a fixed rate to a vacant right neighbor [1–5]. Although simply defined, this model has rich transport properties: for example, density heterogeneities can evolve into rarefaction or shock waves [5], while an open system, with input at one end and output at the other, exhibits a variety of phases as a function of the input/output rates [14–16].

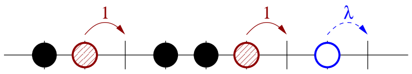

FIG. 1. Cooperative exclusion. A particle can hop to a vacant right neighbor with the rates shown.

A fundamental property of the ASEP is the relation $J(\rho) = \rho(1-\rho)$ between the current J and density ρ. Because each site can be occupied by at most one particle, the average particle velocity $v = J/\rho$ is always a decreasing function of the density. In this work, we investigate a *cooperative exclusion* (CE) model in which cooperativity leads to a velocity that can *increase* with density. Similar cooperativity arises in a variety of systems including ants on a pheromone trail [17, 18], buses on a fixed route [19], molecular motors [20], and even as an underlying cause of superconductivity [21].

In the CE model, a particle can hop to its vacant right neighbor at a rate r that depends on the occupancy of the previous site (Fig. 1):

$$r = \begin{cases} 1 & \text{previous site occupied,} \\ \lambda & \text{previous site vacant,} \end{cases}$$

with $0 \le \lambda \le 1$. When $\lambda = 1$ the standard ASEP is recovered, while $\lambda = 0$ corresponds to *facilitated* asymmetric exclusion [22], in which a particle *must* be "pushed" by a neighboring particle on the left to move to a vacancy on the right. This mechanism was found to give an unexpected rarefaction wave discontinuity [23]. Even more striking, the CE exhibits shock and rarefaction waves that can be continuous, discontinuous, or a mixture of the two. These unusual features arise when $0 < \lambda < \frac{1}{2}$, for which an inflection point in $J(\rho)$ occurs at ρ_I. For $\rho < \rho_I$, interparticle cooperativity dominates, and J grows superlinearly in ρ. At higher density, excluded volume interactions dominate, so that J grows sublinearly and ultimately decreases to zero (Fig. 2). Correspondingly, the group velocity changes from an increasing to a decreasing function of density as ρ passes through ρ_I.

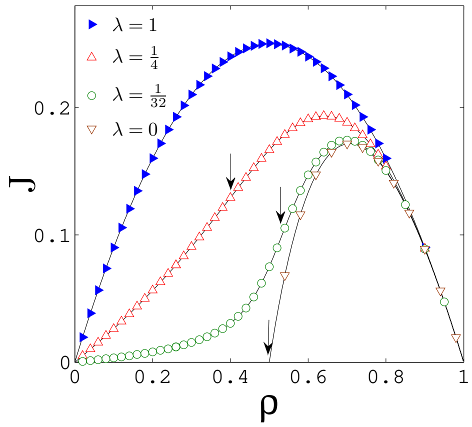

FIG. 2. Steady state current as function of density in cooperative exclusion (CE). Data are based 10^2 realizations with $L = 10^3$ up to $t = 10^4$. The solid curves are given by Eq. (4). Arrows indicate inflection point locations.

For a finite ring of length L that contains N particles (with density $\rho = N/L$), the occupation number n_i equals 1 if i is occupied and 0 otherwise. The set of occupation numbers $\{n_1, \ldots, n_L\}$ subject to particle conservation, $\sum_i n_i = N$, defines a configuration. A crucial feature of CE is that the probability for any steady-state configuration is a decreasing function of the number of adjacent vacancies

$$k \equiv \sum_{i=1}^{L} (1-n_i)(1-n_{i+1})\,, \tag{1}$$

with $n_{L+1} = n_1$. We can understand this result by noting that the hopping of a pushed particle (whose left neighbor is occupied) either preserves ($\bullet\bullet\circ\bullet \to \bullet\circ\bullet\,\bullet$) or decreases ($\bullet\bullet\circ\circ \to \bullet\circ\bullet\,\circ$) the number of adjacent vacancies k. Conversely, the hopping of an isolated particle either preserves ($\circ\bullet\circ\circ \to \circ\circ\bullet\circ$) or increases ($\circ\bullet\circ\bullet \to \circ\circ\bullet\,\bullet$) k. Since pushed particle hopping events occur at a higher rate, configurations with fewer adjacent vacancies are statistically more probable.

We now show that the density distribution is

$$P_k = \frac{\lambda^k}{Z(\lambda)}\ , \tag{2}$$

where P_k is the probability for any configuration that contains k adjacent vacancies and $Z(\lambda)$ is a normalization constant. To verify (2), consider the steady-state detailed balance condition, for which the overall rate of entering and leaving a configuration $\mathcal{C}$ must be equal:

$$P(\mathcal{C})\sum_{\mathcal{C}'} R(\mathcal{C}\to\mathcal{C}') = \sum_{\mathcal{C}'} P(\mathcal{C}')R(\mathcal{C}'\to\mathcal{C})\,. \tag{3}$$

Here $P(\mathcal{C})$ is the probability of configuration $\mathcal{C}$ and $R(\mathcal{C}\to\mathcal{C}')$ is the transition rate from $\mathcal{C}$ to $\mathcal{C}'$. The left side corresponds to all ways of exiting $\mathcal{C}$. There are two contributing processes: either a particle is pushed at rate 1 from a cluster of length ≥ 2, or an isolated particle hops at rate λ. Thus $\sum_{\mathcal{C}'} R(\mathcal{C}\to\mathcal{C}') = G_2 + \lambda c_1$, where G_2 is the number of clusters of length ≥ 2 and c_1 is the number of unit-length clusters in $\mathcal{C}$.

For the right side of (3), we enumerate all events that lead to $\mathcal{C}$. Again, there are two contributing processes. A cluster of length ≥ 2 is created by: (a) $\bullet\bullet\circ\bullet\times \to \bullet\circ\bullet\bullet\times$ or by (b) $\circ\bullet\circ\bullet\times \to \circ\circ\bullet\bullet\times$, where $\times$ indicates any configuration on the right. In (a), the hopping rate is 1 and the relative weights of the initial and final configurations are equal, since the number of vacancy pairs k is unchanged. In (b), the particle hops with rate λ, but the initial configuration has a relative weight $\frac{1}{\lambda}$ according to (2), since the hop increases the number of vacancy pairs by 1. The total weight of these processes is G_2.

Similarly, a unit-length cluster is created by either: (a) $\bullet\bullet\circ\circ \to \bullet\circ\bullet\circ$ or (b) $\circ\bullet\circ\circ \to \circ\circ\bullet\circ$. The first process occurs with rate 1 from a configuration with relative weight λ compared to the final state (since k decreases by 1), while the second occurs with rate λ from a configuration with relative weight 1 (since k is unchanged). The total weight of these processes is λc_1. Thus the sum of the weights of the entrance processes to configuration $\mathcal{C}$ balances those of the exit processes when each configuration has weight proportional to λ^k.

We now make use of the results of Ref. [9], where the steady-state distribution P_k was shown to coincide with the equilibrium distribution of a one-dimensional Ising model. Using standard transfer-matrix techniques, the average current between sites i and $i+1$,

$$\begin{aligned} J &= \mathrm{Prob}(\bullet\bullet\circ) + \lambda\mathrm{Prob}(\circ\bullet\circ) \\ &= \langle [n_{i-1} + \lambda(1-n_{i-1})]\, n_i(1-n_{i+1})\rangle\,, \end{aligned}$$

may be shown to be

$$J = (1-\rho)\left[1 + \frac{\sqrt{1-4(1-\lambda)\rho(1-\rho)}-1}{2(1-\lambda)\rho}\right] \tag{4}$$

in the $L\to\infty$ limit. The salient feature of this expression for J is the existence of an inflection point at a density ρ_I for $\lambda < \frac{1}{2}$ (Fig. 2). We henceforth restrict our analysis to this domain and investigate the unusual consequences that follow.

Specifically, we focus on the evolution from the step initial condition

$$\rho(x,t=0) = \begin{cases} \rho_- & x\leq 0\,,\\ \rho_+ & x>0\,. \end{cases} \tag{5}$$

In a hydrodynamic theory, the particle density satisfies the continuity equation

$$\rho_t + J_x = 0\,. \tag{6}$$

By the chain rule, we rewrite the second term as $J_\rho\,\rho_x$, from which the group velocity $u = J_\rho$ (here and henceforth the subscripts x,ρ denote partial differentiation). Because of the inflection point in $J(\rho)$, the group velocity can be either an increasing or decreasing function of ρ. The difference in the group velocity to the right and left of the initial density upstep ($\rho_- < \rho_+$) or downstep ($\rho_- > \rho_+$) determines whether a continuous, discontinuous, or a mixed density profile emerges. On length and time scales that are large compared to microscopic scales, we can use the steady-state expression (4) for the current to determine these non-steady state profiles.

Shock/Inverted Shock: In the conventional ASEP, an upstep evolves to a shock because the group velocity $u(\rho_-)$ in the low-density region on the left exceeds the velocity $u(\rho_+)$ in the high-density region on the right. Thus particles pile up at the interface to form a shock wave, much like freely-moving cars that approach a traffic jam. This situation also occurs in CE in the "normal" range $\rho_I < \rho_- < \rho_+$, where exclusion dominates and $u(\rho_-) > u(\rho_+)$. However, when $\rho_+ < \rho_- < \rho_I$, then $J_{\rho\rho} = u_\rho > 0$ — the group velocity is an increasing function of the density. Even though there is a downstep, the group velocities still obey $u(\rho_-) > u(\rho_+)$ because of the cooperativity. Thus particles in the high-density region on the left again overtake and pile up at the interface. We term this singularity an *inverted shock (IS) wave* (Fig. 3).

For both shocks and inverted shocks, the density profile is given by $\rho = \rho(x-ct)$. We find the shock speed c by equating the net flux into a large region that includes the shock, $J(\rho_+) - J(\rho_-)$, with the change in the number of particles, $c(\rho_+ - \rho_-)$, in this region to give the standard expression [24]

$$c = \frac{J(\rho_+) - J(\rho_-)}{\rho_+ - \rho_-} \ . \tag{7}$$

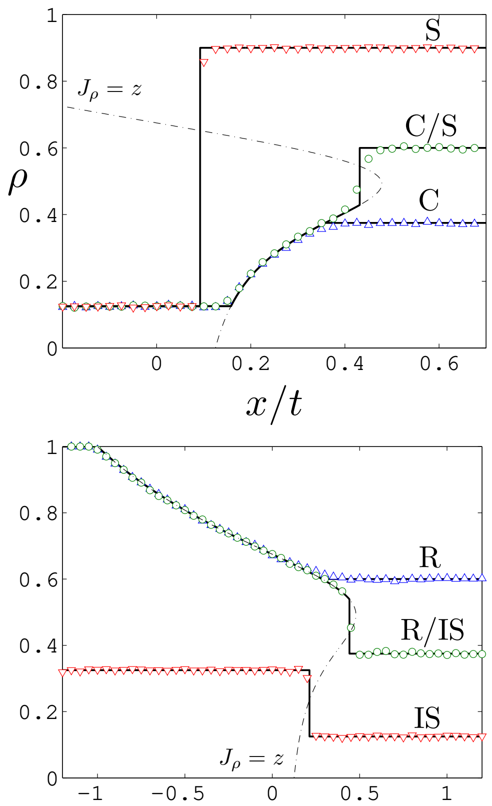

FIG. 3. (top) Evolution of an upstep for $\lambda = \frac{1}{8}$: (C) continuous compression wave for $\rho_- = \frac{1}{8}$, $\rho_+ = \frac{3}{8}$; (C/S) mixed compression/shock for $\rho_- = \frac{1}{8}$, $\rho_+ = 0.6$; (S) shock for $\rho_- = \frac{1}{8}$, $\rho_+ = 0.9$. (lower) Evolution of a downstep for $\lambda = \frac{1}{8}$: (R) continuous rarefaction for $\rho_- = 1$, $\rho_+ = 0.6$; (R/IS) mixed rarefaction/inverted shock for $\rho_- = 1$, $\rho_+ = \frac{3}{8}$; (IS) inverted shock for $\rho_- = 0.325$, $\rho_+ = \frac{1}{8}$. The dashed line is the locus $J_\rho = z$ and the solid black curves are analytic predictions. Simulations are based on 10^3 realizations up to $t = 4 \times 10^3$.

Continuous Rarefaction/Compression: A downstep always evolves to a continuous rarefaction wave in the ASEP because particles in the leading low-density region move forward quickly, leaving open space for the initial downstep to smooth out, similar to stopped cars spreading apart after a stoplight turns green. The same qualitative behavior also occurs in CE when the initial densities satisfy $\rho_I < \rho_+ < \rho_-$. Here, the group velocity is a decreasing function of density, so that the leading low-density particles move the fastest. However, when the initial densities satisfy $\rho_- < \rho_+ < \rho_I$, the group velocity in the high-density regime exceeds that in the low-density regime. Thus instead of a shock wave, the system develops a *continuous compression (C) wave* (Fig. 3).

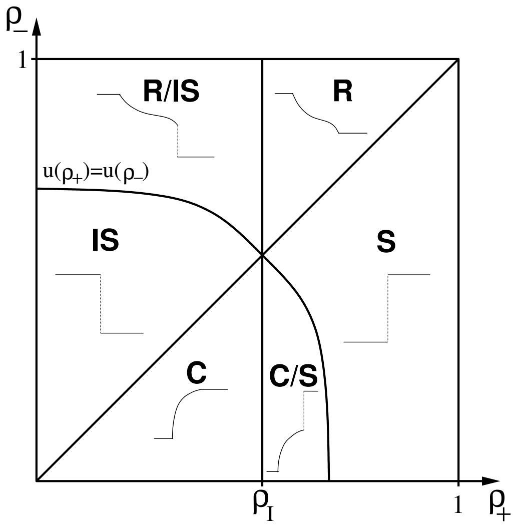

FIG. 4. Phase diagram of the CE model for an initial density step (ρ_-, ρ_+), with ρ_I the inflection point in $J(\rho)$. A typical density profile $\rho(z)$ is sketched for each of the six regions: (R/IS) rarefaction/inverted shock, (R) continuous rarefaction, (S) shock, (C/S) compression/shock, (C) continuous compression, (IS) inverted shock.

To determine the density profile, we assume that the density is a function of the scaled variable $z = x/t$. Substituting $\rho(x,t) = \rho(z)$ into the continuity equation (6), we find that the profile consists of segments where the density is either constant or else satisfies $z = J_\rho$. Matching these solutions gives [6, 23]

$$\rho(z) = \begin{cases} \rho_- & z < z_- \ , \\ I(z) & z_- \le z \le z_+ \ , \\ \rho_+ & z > z_+ \ , \end{cases} \tag{8}$$

where $I(z)$ is the inverse function of $z = J_\rho$. For a continuous profile, the cutoffs z_- and z_+ satisfy $I(z_\pm) = \rho_\pm$, which are equivalent to $z_\pm = J_\rho(\rho_\pm)$.

Mixed Rarefaction/Compression and Shock: It is also possible for continuous rarefaction/compression to coexist with a shock. Starting with a downstep, coexistence arises when $\rho_+ < \rho_I < \rho_-$, but with ρ_+ close to ρ_I, so that $u(\rho_-) < u(\rho_+)$ — the velocity on the right exceeds that on the left. Qualitatively, the leading particles race ahead to smooth out the downstep. Since the density at the leading edge gradually decreases, the cooperative interaction weakens. Eventually, the velocity of the leading particles decreases to the point where particles pile up behind. In this way, the leading edge of the rarefaction wave terminates in an inverted shock.

Similarly, an upstep can evolve to a compression wave with a leading shock when $\rho_- < \rho_I < \rho_+$ and $u(\rho_-) < u(\rho_+)$. High-density particles now move faster than those in the low-density region. However, because $u_\rho < 0$, the density at the leading edge increases along with excluded volume interactions until the velocity is less than that of trailing particles and a pileup (shock) occurs. The variety of phases that arise from an initial density step are illustrated in Fig. 4. For the ASEP, the corresponding phase diagram consists of only continuous rarefaction and shock wave solutions; there is no analog of the rarefaction/inverted shock and compression/shock profiles.

The functional form of the rarefaction/inverted shock and compression/shock profiles are still given by Eq. (8), but the criteria to determine the cutoffs $z_\pm$ are now more involved than for continuous profiles. The left cutoff, z_-, is still determined by continuity, namely, $I(z_-) = \rho_-$ or, alternatively, $z_- = J_\rho(\rho_-)$. To determine the right cutoff z_+, we note that in a small spatial region that includes the leading discontinuity, the density profile is just that of a shock or inverted shock wave. Thus we may adapt Eq. (7) for the shock wave speed and obtain

$$z_+ = \frac{J(q_+) - J(\rho_+)}{q_+ - \rho_+}\,, \tag{9}$$

where $q_+ \equiv I(z_+)$ is the density immediately before the discontinuity. (Note also that $z_+ = J_\rho(q_+)$ by definition.)

To justify (9), we use the particle conservation equation that the number of particles in $[z_-, z_+]$ equals the initial number plus the net flux into this region:

$$\int_{z_-}^{z_+} I(z)dz = -\rho_- z_- + \rho_+ z_+ - J(\rho_+) + J(\rho_-)\,. \tag{10}$$

We recast this expression into (9), by making the variable change $z = J_\rho(\rho)$ and using $I(J_\rho(\rho)) = \rho$ to write the integral as $\int_{\rho_-}^{q_+} \rho\, J_{\rho\rho}\, d\rho$, which can be performed by parts. The resulting expression readily simplifies to (9).

In summary, rich behavior arises in *cooperative exclusion* due to the existence of an inflection point at ρ_I in the current-density relation $J(\rho)$. As a consequence, the group velocity is an *increasing* function of density for $\rho < \rho_I$, a dependence opposite to that in the conventional ASEP. The resulting non-monotonic density dependence of the velocity leads to an unusual evolution of density upsteps and downsteps. These configurations can evolve to: (i) shock/inverted shocks, (ii) continuous rarefaction/compression waves, or (iii) a mixed profile that contains both continuous and discontinuous elements.

We thank Martin Schmaltz for asking an oral exam question that helped spark this work and Paul Krapivsky for helpful discussions. We also gratefully acknowledge financial support from NSF grant DMR-0906504.

[1] B. Schmittmann and R. K. P. Zia, in *Phase Transitions and Critical Phenomena*, Vol. 17, eds. C. Domb and J. L. Lebowitz (Academic Press, London, 1995).
[2] B. Derrida, Phys. Repts. **301**, 65 (1998); J. Stat. Mech. P07023 (2007).
[3] T. M. Liggett, *Stochastic Interacting Systems: Contact, Voter, and Exclusion Processes* (Springer, New York, 1999).
[4] G. Schütz, in *Phase Transitions and Critical Phenomena*, Vol. 19, eds. C. Domb and J. L. Lebowitz (Academic Press, London, 2000).
[5] R. A. Blythe and M. R. Evans, J. Phys. A **40**, R333 (2007).
[6] P. L. Krapivsky, S. Redner, and E. Ben-Naim, *A Kinetic View of Statistical Physics* (Cambridge University Press, Cambridge, 2010).
[7] K. Klauck and A. Schadschneider, Physica A **271**, 102 (1999).
[8] V. Popkov and G. M. Schütz, Europhys. Lett. **48**, 257 (1999).
[9] T. Antal and G. M. Schütz, Phys. Rev. E **62**, 84 (2000).
[10] A. Schadschneider, D. Chowdhury, and K. Nishinari, *Stochastic Transport in Complex Systems: From Molecules to Vehicles*, (Elsevier, 2010).
[11] P. M. Richards, Phys. Rev. B **16**, 1393 (1977).
[12] C. T. MacDonald, J. H. Gibbs, and A. C. Pipkin, Biopolymers **6**, 1 (1968).
[13] C. T. MacDonald and J. H. Gibbs, Biopolymers **7**, 707 (1969).
[14] J. Krug, Phys. Rev. Lett. **67**, 1882 (1991).
[15] B. Derrida, E. Domany, and D. Mukamel, J. Stat. Phys. **69**, 667 (1992).
[16] G. M. Schütz and E. Domany, J. Stat. Phys. **72**, 277 (1993).
[17] M. Burd, D. Archer, N. Aranwela, and D. J. Stradling, Am. Nat. **159**, 283 (2002)
[18] D. Chowdhury, A. Schadschneider, and K. Nishinari, Phys. Life Rev. **2**, 318 (2005).
[19] O. J. O'Loan, M. R. Evans, and M. E. Cates, Phys. Rev. E **58**, 1404 (1998).
[20] D. Chowdhury, Physica A **372**, 84 (2006).
[21] W. A. Little, Phys. Rev. Lett. **134**, A1416 (1964); Sci. Am. **212**, 21 (1965).
[22] U. Basu and P. K. Mohanty, Phys. Rev. E **79**, 041143 (2009).
[23] A. Gabel, P. L. Krapivsky, and S. Redner, Phys. Rev. Lett. **105**, 210603 (2010).
[24] G. B. Whitham, *Linear and Nonlinear Waves* (Wiley, New York, 1974).